Investigation of NH3/CH4 Flame Structure and Dynamics in a Swirl Turbulent Non-Premixed Burner

Antoine Morel and Toufik Boushaki

ICARE-CNRS, University of Orleans, Orléans, France

1 Introduction

The transition to sustainable and cleaner energy sources has become a critical priority in addressing current environmental challenges. One promising energy carrier is ammonia (NH3), which offers high energy density, ease of transportation, and a carbon-free composition. However, its low flame speed, limited calorific value, combustion instability, and high NOx emissions present significant challenges for achieving efficient combustion (Kobayashi et al. [1], Valera-Medina et al. [2]). To overcome these limitations, blends of ammonia and methane (CH4) are being studied as a viable alternative. Methane, which can be derived from biomass sources, is well-researched and provides higher reactivity to improve flame stability (Elbaz et al. [3], Ariemma et al. [4], Wang et al. [5]). However, in non-premixed swirling flame configurations, the complex interactions between the reactants, flow dynamics, and stabilization mechanisms require detailed analysis to fully understand and control flame behavior. Among the techniques used to influence and modify flame characteristics, radial fuel injection in swirling configurations has shown great potential to impact flame structure and stability (Chakchak et al. [6], Mansouri and Boushaki [7]). Despite this, the specific mechanisms governing flame structure and stabilization in NH3/CH4 blends remain largely unexplored. In this context, the present study investigates the flame stabilization mechanisms in non-premixed swirling flames fueled by NH3/CH4 blends, with a radial fuel injection. Chemiluminescence on OH* and NH2*, NOx emissions and flow field measurements were performed for methane "as a reference case", and NH3-CH4 mixtures of 50-50, 60-40 and 90-10%, under constant total flow rates or constant flame power, offering insights into the mechanisms driving flame shaping.

2 Experimental Setup

Figure 1 shows the experimental setup used for this study. The swirl burner with radial fuel injection is shown on Figure 1 a.. The burner is composed of 2 concentric parts with a central tube of 15 mm in diameter corresponding to fuel (ammonia and methane) injection and an annular part of 38 mm inner diameter corresponding to air injection.

The radial fuel injector is composed of 8 holes with 3 mm in diameter. The swirler is placed in the annular part at $h = 50mm$ from the burner's outlet, which geometrical swirl number is fixed to $Sn = 0.8$.

Correspondence to: antoine.morel@cnrs-orleans.fr

The experimental setup features a combustion chamber with a stainless-steel square base measuring $48 \times 48cm^2$ and a height of 1 meter, designed to operate at atmospheric pressure. The chamber's walls and base are externally cooled by water and internally lined with 10 mm thick refractory panels. Optical access to the flame is provided by 24 observation windows, distributed as six per side. The exhaust section incorporates a convergent outlet with a diameter of 10 cm, ensuring the evacuation of flue gases via a ventilation duct to prevent gas stagnation within the chamber.

Three measurement techniques are used. The first, dedicated to chemiluminescence imaging (Figure 1 b.), is used to characterize flame fronts and fluctuations. It employs a PI-MAX 4 ICCD camera equipped with a UV lens and specific wavelength filters. Mounted on a 3D translation stage, the camera is positioned to capture the burner outlet, optimizing the observation area. Flame-emitted light passes through the filter to the camera, and the data is processed via a controller and acquisition computer. For each condition, 200 instantaneous images with a 5 ms exposure time were averaged. Chemiluminescence focused on two radicals: OH*, indicative of CH4-air combustion, and NH2*, representing ammonia oxidation. Bandpass filters were used for precise detection: 310 nm (5 nm FWHM) for OH* and 632 nm (5 nm FWHM) for NH2*. In addition to capturing chemiluminescence data, direct photographs of the flame were taken to visually compare its appearance with the chemiluminescence findings. These images were captured using a CANON EOS 77D camera equipped with an EFS 18-55mm lens and an exposure time of 1/8 s.

The second experimental setup is dedicated to Laser Doppler Anemometry (LDA) for measuring the axial velocity component in reactive flows with high precision (Figure 1 c.). The TR-SS-2D Laser Doppler Velocimetry (LDV) system, based on solid-state lasers, comprises a PowerSight probe, a PDM1000 signal filtering module, and an FSA3500 signal processor for data acquisition and analysis. In this study, only laser beams with a wavelength of 561 nm are utilized. These beams intersect at the focal point, creating an ellipsoidal measurement volume where particle velocities are accurately determined using the Doppler effect. A 350 mm focal length lens is used to focus the laser beams, ensuring precise beam convergence at the measurement volume. To prevent thermal expansion due to proximity to the flame, the lens is cooled to 298 K. Zirconium oxide (ZrO2) tracer particles, known for their high melting point and resistance to elevated temperatures, are used to ensure reliable measurements in the combustion environment. These particles are preheated to 383 K to minimize agglomeration. The resulting Doppler signals are processed to compute velocities with an accuracy of better than 0.5%. A high-precision 3D positioning system, identical to the one used in the chemiluminescence setup, is employed to align the laser relative to the burner. This system provides a positioning resolution of 0.1 mm, enabling detailed mapping of the flow field. The measurements were performed along five horizontal lines intersecting the burner's symmetrical axis at heights of 2 mm, 10 mm, 20 mm, 38 mm, and 60 mm. These heights were selected to correspond to the flame's location, ensuring a comprehensive representation of the flow field.

Finally, the third setup (Figure 1 d.) consists of a gas analyzer (ECOM-J2KN + HORIBA PG250) designed to measure NOx emissions in the flue gases exiting the combustion chamber. The NOx concentrations were determined using an electrochemical cell. To prevent water vapor condensation, the gas sampling lines were electrically heated. The gas sampling probe was positioned 120 cm downstream of the burner exit. The uncertainties associated with the flue gas measurements are estimated to be approximately 3% of the measured concentration.

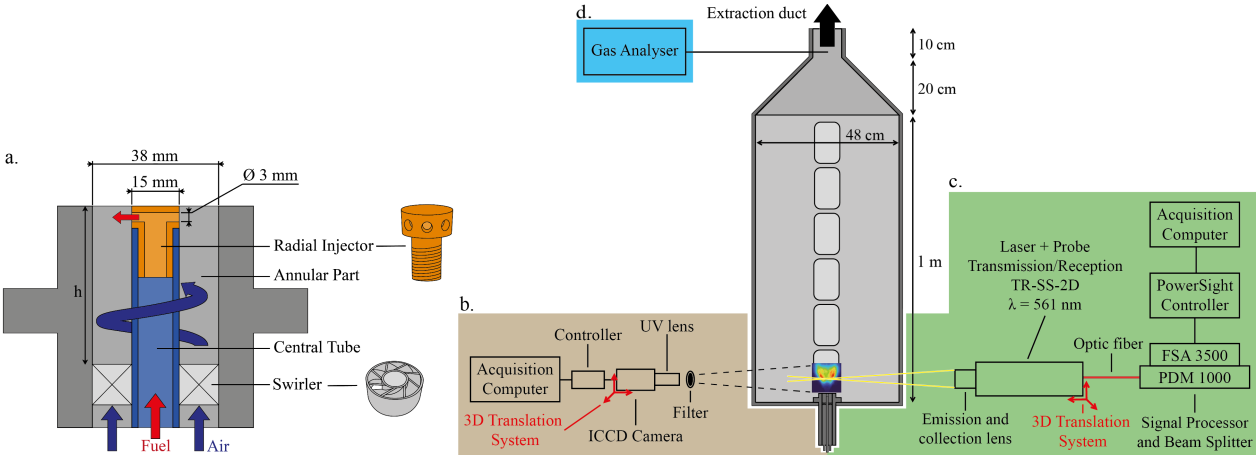

Figure 1: Schematic view of the experimental setup. a) Swirl burner with radial fuel injection, b) chemiluminescence technique setup, c) LDA measurement setup, d) Flue gases analysis setup.

3 Results and Discussions

The experiments were conducted under atmospheric conditions, focusing on four specific cases. The first case served as a reference, featuring a pure methane flame operating at a power of 10 kW (called Ref0NH3). The second case represented an extreme condition near flame extinction, with 90% ammonia in the fuel mixture at 10 kW (called Ext90NH3). The remaining two cases involved "steady" dynamics, characterized by constant fuel and air flow rates at approximately 10 kW (called Dyn50NH3 and Dyn60NH3). These latter cases were of particular interest due to an observed change in the flame's shape under these conditions. Table 1 summarizes the parameters (equivalence ratio Φ, Swirl number Sn, flame power P and flow rates Q) corresponding to the four cases.

Table 1: Operating conditions.

Case	$\%NH3$	ϕ	Sn	P (kW)	Q_{fuel} (l/mn)	Q_{CH4} (l/mn)	Q_{NH3} (l/mn)	Q_{air} (l/mn)
Constant power								
Ref0NH3	0	1.0	0.8	10	17.64	17.64	0	167.76
Ext90NH3	90	1.0	0.8	10	38.38	3.84	34.54	159.51
Constant flow rates								
Dyn50NH3	50	0.8	0.8	10.9	27.58	13.79	13.79	204.7
Dyn60NH3	60	0.8	0.8	10	27.58	11.03	16.55	204.7

Figure 2 presents flame imaging for the four cases. The direct photographs reveal distinct flame shapes and colors depending on the operating conditions. The yellow hue corresponds to ammonia combustion via NH2* and H2O* signals, while the blue hue indicates complete methane combustion. The chemiluminescence results highlight that the shape and location of OH* and NH2* production zones are strongly influenced by the flame dynamics. Specifically, when the flame is attached to the burner, the OH* and NH2* production zones tend to separate. Conversely, when the flame is lifted, these production zones exhibit almost identical shapes. As observed in the direct photographs for the Dyn50NH3 and Dyn60NH3 cases, this

separation underscores the significant impact of burned gas recirculation on flame chemistry, which may explain the subtle shift in the base color of the flame. Furthermore, the Dyn50NH3 and Dyn60NH3 cases are characterized by constant inlet fuel and air flow rates, with the only variable being the ammonia proportion in the fuel. The observed changes in flame shape suggest that ammonia properties are a critical factor in flame behavior. A likely explanation is that ammonia's lower adiabatic flame temperature and flame burning velocity compared to methane reduces the overall flame temperature as its proportion increases. These parameters reduction alters the flame chemistry and subsequently influences the flow dynamics.

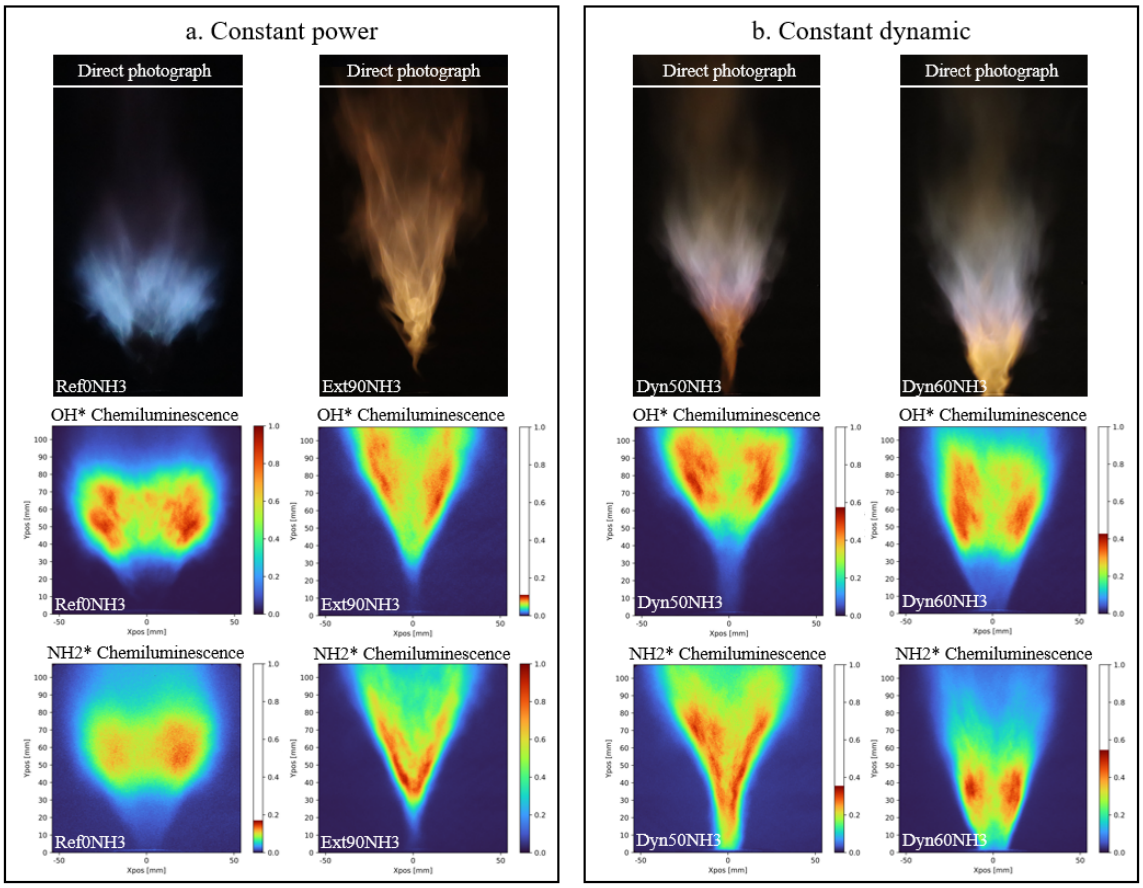

Figure 2: Direct photograph and chemiluminescence of OH* and NH2* radicals for the studied cases.

Table 2 summarizes the lift-off height for the four cases, measured from chemiluminescence images of OH and NH2 radicals. Each lift-off height is presented with its respective standard deviation. These measurements provide insight into the overlap between radical production zones.

For the constant power cases, the production zones of OH* and NH2* radicals exhibit moderate overlap when considering the standard deviation, with an average difference of approximately 10 mm between the two radicals across both cases. Globally, the lift-off height in the Ext90NH3 case is lower than in the Ref0NH3 case.

In the constant dynamic cases, significant differences are observed. The Dyn50NH3 case shows a much higher lift-off height compared to Dyn60NH3, with an average difference of 15 mm for the NH2* radical and 17 mm for the OH* radical. When comparing the two radicals, a clear separation between their production

zones of approximately 30 mm is observed. This separation likely explains the noticeable difference in flame color, as shown in Figure 2b.

Table 2: Lift off height measurements.

	Constant power		Constant dynamic	
Case	Ref0NH3	Ext90NH3	Dyn50NH3	Dyn60NH3
OH* chemiluminescence				
L off (mm)	35.8 ± 3.9	43.1 ± 5.8	52.4 ± 5.1	35.0 ± 4.8
NH2* chemiluminescence				
L off (mm)	42.2 ± 4.4	31.3 ± 6.5	19.4 ± 10.1	4.8 ±7.8

Figure 3 presents the axial velocity results with the inverse Abel transform of OH* chemiluminescence for the Ref0NH3 and Ext90NH3 cases. While multiple cases were analyzed during this study, the results of two representative cases are presented here for conciseness. The full dataset confirms the trends and conclusions discussed in this work and is available for further exploration.

A key observation is the difference in recirculation zones between the two cases. Furthermore, the flame location, as identified by the inverse Abel transform of OH* chemiluminescence, differs significantly. In the Ref0NH3 case, the flame is primarily located between the flow disturbance limit and the maximum velocity line, whereas in the Ext90NH3 case, it is situated between the direction change boundary and the maximum velocity line. This can be attributed to methane's ability to sustain higher flow velocities and the shape of the recirculation zone, which allows for a broader flame.

The intensity of negative velocities is higher in the Ext90NH3 case, explaining the reduced lift-off height compared to Ref0NH3. Additionally, the cross-flow effect resulting from radial injection is noticeable in the velocity profiles. In the Ext90NH3 case, the doubled fuel flow rate compared to Ref0NH3 leads to a slight expansion of the negative velocity zone in the 2 mm profile and a reduction in the velocity maxima across all profiles. Furthermore, the increased flow rate enhances the momentum, resulting in a more pronounced depression in the central recirculation zone above the burner.

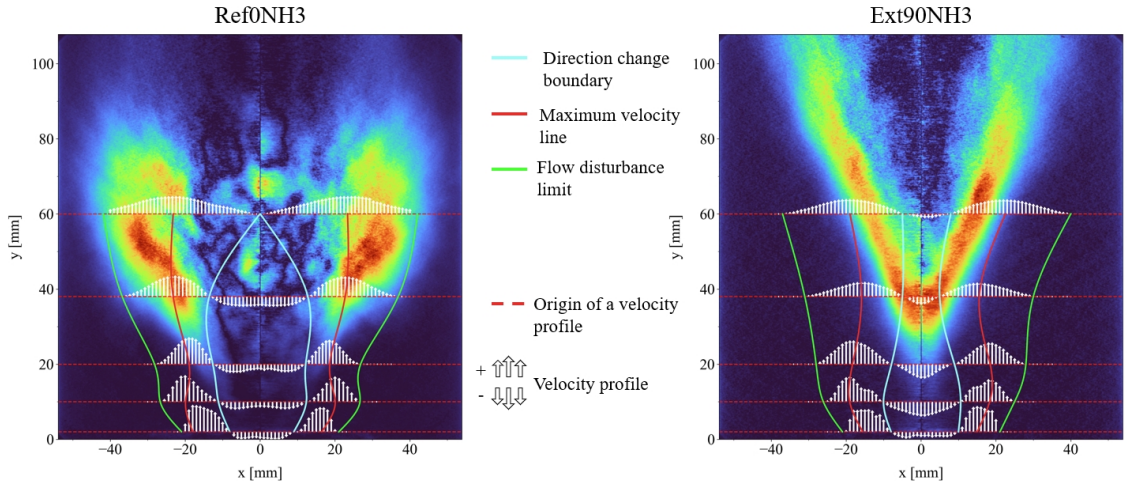

Figure 3: Axial velocity measurements and inverse Abel transform of OH* chemiluminescence for Ref0NH3 and Ext90NH3 cases.

4 Conclusion

In the present work, the axial velocity and OH* and NH2* chemiluminescence of methane and ammonia mixture was investigated. This study highlights the influence of operating conditions and fuel composition on flame dynamics and chemistry in ammonia-methane combustion. Chemiluminescence analysis revealed that the stabilization zone and location of OH* and NH2* production zones are strongly influenced by the recirculation of burned gases, which affects flame stability and coloration. The differences in flame shape and lift-off height between cases are attributed to the distinct physical and chemical properties of methane and ammonia, including their respective flame burning velocity and potentially their adiabatic flame temperature.

Furthermore, axial velocity measurements showed the critical role of recirculation zone intensity and radial injection on the velocity profiles and flame positioning. Increasing ammonia content significantly altered the velocity distribution, increased negative velocity zones, and reduced lift-off heights, emphasizing the impact of ammonia's lower flame burning velocity. These findings demonstrate the interaction between flow dynamics and fuel composition, offering valuable insights for optimizing ammonia-methane combustion systems under varying operating conditions.

5 Acknowledgements

The authors are grateful for the financial support of this work provided by Valormac JRP CNRS-Africa and LEAP RE Biotherap.

References

[1] Kobayashi H, Hayakawa A, Somarathne K, Okafor E. (2020) Science and technology of ammonia combustion. Proc. Combust. Inst. 1186:1205.

[2] Valera-Medina A, Amer-Hatem F, Azad A, Dedoussi I, de Joannon M, Fernandes R, Glarborg P, Hashemi H, He X, Mashruk S, McGowan J, Mounaim-Roouselle C, Ortiz-Prado A, Ortiz-Valera A, Rossetti I, Shu B, Yehia M, Xiao H, Costa M. (2021) Review on Ammonia as a Potential Fuel: From Synthesis to Economics. Energy & Fuels. 6964:7029.

[3] Elbaz A, Hassan Z, Robert W. (2024) Exploring the influence of swirl intensity on stability, emissions, and flame structure in non-premixed NH3/CH4 swirling flames. Proc. Combust. Inst. 105644.

[4] Ariemma G, Sorrentino G, Ragucci R, de Joannon M, Sabia P. (2022) Ammonia/Methane combustion: Stability and NOx emissions. Combustion and flame. 112071.

[5] Wang J, Jiang X, Luo K. (2023) Exploring reaction mechanism for ammonia/methane combustion via reactive molecular dynamics simulations. Fuel. 125806.

[6] Chakchak S, Hidouri A, Zaidaoui H, Chrigui M, Boushaki T. (2021) Experimental and numerical study of swirling diffusion flame provided by a coaxial burner: Effect of inlet velocity ratio. Fluids. 159.

[7] Mansouri Z, Boushaki T. (2018) Experimental and numerical investigation of turbulent isothermal and reacting flows in a non-premixed swirl burner. International Journal of Heat and Fluid Flow. 200:213.

[8] Boushaki T, Merlo N, Chauveau C, Gökalp I. (2017) Study of pollutant emissions and dynamics of non-premixed turbulent oxygen enriched flames from a swirl burner. Proc. Combust. Inst. 3959:3968.